**Proceedings of the 7th GACM Colloquium on Computational Mechanics
for Young Scientists from Academia and Industry
October 11-13, 2017 in Stuttgart, Germany**

A homogenization approach for beam-like structures with arbitrarily shaped and deformable cross-sections

Simon Klarmann[1]* and Friedrich Gruttmann[1]

Micro Abstract
Beam elements demonstrate an efficient way of modeling large, thin structures if the assumed kinematics are reasonable. Regarding arbitrarily shaped cross-sections and varying material properties, difficulties arise in describing their behavior. A homogenization approach for a simple Timoshenko beam using a representative volume element circumvents this problem. In addition to that cross-sectional deformations can be taken into account.

[1]Solid Mechanics, Technical University of Darmstadt, Darmstadt, Germany
***Corresponding author**: klarmann@mechanik.tu-darmstadt.de

Introduction

Recently numerical homogenization schemes are widely used to model large structures while taking the behavior of the micro structure into account. The calculation is then carried out with the so called FE^2 approach, meaning a second FE calculation is performed to get homogenized material properties as well as stresses. Regarding the homogenization theory the Hill condition is the most common approach and is well investigated when coupling scales with a full 3D stress and strain state. However, the resulting workload is massive because even with the lowest order 3D element, eight RVEs per element need to be evaluated. A drastic reduction of this workload can be achieved by using degenerated elements like beams, plates or shells. In this work beam elements are considered, which leads to an evaluation of only one RVE per element. The main goal is to recover the 3D stress state. This approach has already been used, mainly for shell elements, but there is still a severe problem considering the shear deformation state. Here, the coupling between shear force and bending moment distribution leads to a length dependency of the RVE. This problem will be investigated and a possible solution is given as well as tested on appropriate numerical examples.

1 Homogenization scheme

In order to perform the homogenization, macro strains have to be applied onto the micro scale. Since homogenized values contain information about the cross-section, it is more appropriate to talk about a meso scale. Here, coupling is performed for the Timoshenko beam assumptions with the strain tensor $\boldsymbol{\varepsilon} = [\varepsilon, \gamma_y, \gamma_z, \kappa_x, \kappa_y, \kappa_z]$. These strains have to be transferred onto the RVE, therefore it is necessary to look at the equation system of one RVE

$$\frac{1}{l_i}\delta\mathbf{V}_i^T\left(\mathbf{K}_i^L\Delta\mathbf{V}_i + \mathbf{F}_i^L\right) = \frac{1}{l_i}\sum_{e=1}^{N}\begin{bmatrix}\delta\mathbf{v}_a\\ \delta\mathbf{v}_b\end{bmatrix}\left\{\begin{bmatrix}\mathbf{k}_{aa} & \mathbf{k}_{ab}\\ \mathbf{k}_{ba} & \mathbf{k}_{bb}\end{bmatrix}\begin{bmatrix}\Delta\mathbf{v}_a\\ \Delta\mathbf{v}_b\end{bmatrix} + \begin{bmatrix}\mathbf{f}_a\\ \mathbf{f}_b\end{bmatrix}\right\}. \qquad (1)$$

Degrees of freedom are already separated into free ($\mathbf{v}_a$) and fixed ($\mathbf{v}_b$) ones. Then the macroscopic strains are related to $\mathbf{v}_b$ with

$$\mathbf{v}_b = \mathbf{A}\boldsymbol{\varepsilon} \qquad \delta\mathbf{v}_b = \mathbf{A}\delta\boldsymbol{\varepsilon} \qquad \Delta\mathbf{v}_b = \mathbf{A}\Delta\boldsymbol{\varepsilon}. \qquad (2)$$

For the Timoshenko beam theory the matrix $\mathbf{A}$ reads

$$\mathbf{A} = \begin{bmatrix} x & 0 & 0 & 0 & xz & -xy \\ 0 & x & 0 & -xz & 0 & 0 \\ 0 & 0 & x & xy & 0 & 0 \end{bmatrix}. \tag{3}$$

Further details regarding evaluation of stresses and linearized stresses can be found in [2].

2 Boundary Conditions

As outlined in sec. 1, two scales, macro and meso scale, are coupled by transferring the beam strains onto the latter. These strains are an average of the cross-sectional ones. Therefore suitable boundary conditions (b.c.) need to be found to allow a deviation from a plane cross-section.

2.1 Problem: Shear deformation

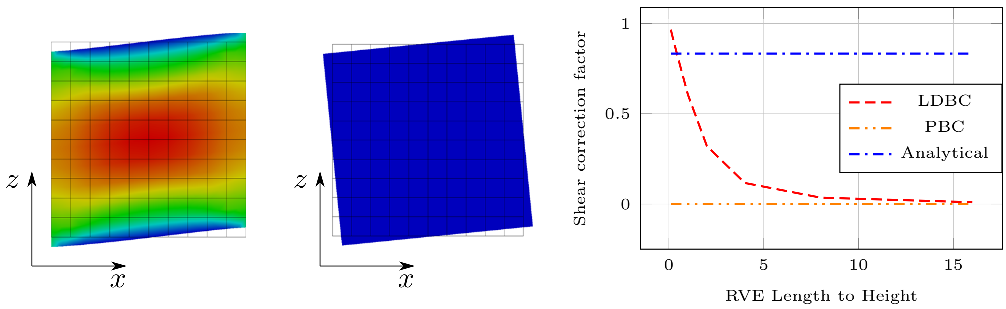

(a) Linear disp. b.c. **(b)** Periodic b.c. **(c)** Influence RVE length

Figure 1. Shear deformation of the RVE and length dependency

At this point it is worth mentioning that periodic b.c. (PBC) lead to perfect results regarding tension, bending and torsion (applied to the center of shear). But fail to give any results for the shear stiffness, see fig. 1b. One way to circumvent this problem is to apply linear displacement b.c. (LDBC) in length direction of the RVE, see fig. 1a. With these, two problems arise. The first one is that the cross-section stays plane, which leads to some boundary effects. But as long as the RVE is long enough, it has no impact on the results. A more severe problem is depicted in fig. 1c. The diagram shows the resulting shear correction factor when varying length with respect to height of the RVE ($\frac{l}{h}$). As mentioned before, PBC lead to a shear correction factor of zero. And in case of LDBC the shear correction factor is length dependent converging against the solution of PBC with increasing ratio $\frac{l}{h}$. Therefore a conflict in choosing the correct length for the RVE arises between a high value of $\frac{l}{h}$ to reduce the influence of boundary effects and a low ratio $\frac{l}{h}$ to get a suitable shear correction factor (in fig. 1c $\frac{l}{h} \approx 0.5$ for the analytical solution). The reason for the length dependency of the shear stiffness can be found in fig. 2. In this case a shear deformation leads to a constant shear force and a linear moment distribution.

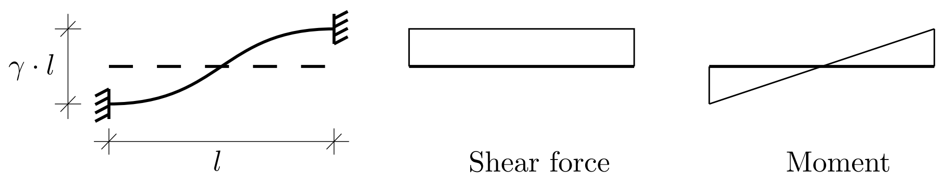

Figure 2. Beam shear deformation and stress resultant

2.2 Additional constraints

The objective is to remove the length dependency and make PBC usable. Regarding the length dependency it is necessary to let the linear moment distribution vanish. Here, two possibilities are regarded. The first one is to set the warping displacements constant over the length, which can be achieved by linking all displacement increments in x-direction onto one surface. This requires that each node must have one corresponding node on the surface. The second possibility is to remove the linear distribution of moment in an average sense, leading to a constraint

$$\int_{RVE} \boldsymbol{\sigma}_n \cdot (y \cdot \boldsymbol{\lambda}_z + z \cdot \boldsymbol{\lambda}_{\boldsymbol{y}}) \ \mathrm{d}V = 0, \tag{4}$$

where $\boldsymbol{\sigma}_n = [\sigma_x, \sigma_y, \sigma_z]$, $\boldsymbol{\lambda}_y = [\lambda_{y1}, \lambda_{y2}, \lambda_{y3}]$ and $\boldsymbol{\lambda}_z = [\lambda_{z1}, \lambda_{z2}, \lambda_{z3}]$. All λ are functions of the length direction x and equal, in shape, the moment distribution resulting from a shear deformation with respect to the boundary conditions. In total these are additional 6 constraints.

To make PBC usable the second constraint has to remove rigid body rotation in case of shear deformation. The idea is to apply an interface element in the center of the RVE and set its rotation to zero in an average sense. This leads to

$$\int_V (\sigma_x - \overline{\sigma}_x) (y \cdot \mu_z + z \cdot \mu_y) \ \mathrm{d}V. \tag{5}$$

For both, σ_x and $\overline{\sigma}_x$, linear elasticity is assumed. The difference between them lies in the evaluation of the strains. Here, σ_x is evaluated in a standard manner, while for $\overline{\sigma}_x$, diplacements u_x^S of the surface are replaced by the product of two angles and the distance to the center of gravity, $u_x^S = \varphi_y \cdot \overline{z} + \varphi_z \cdot \overline{y}$. The Lagrangian parameter μ_y and μ_z enforce this balance in an average sense. With the above given additional constraints, the RVE is structured like in fig. 3.

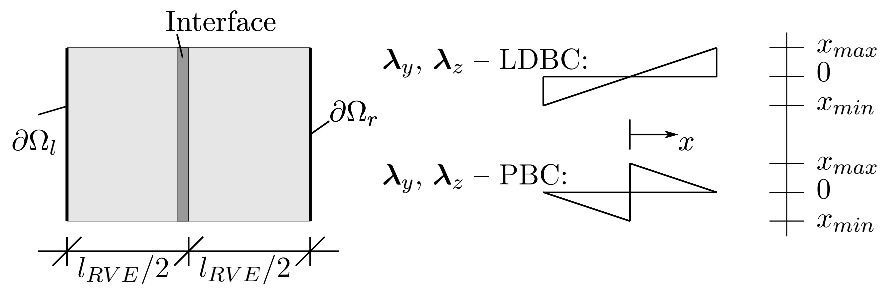

Figure 3. RVE and functions for $\boldsymbol{\lambda}$ in eq. (4)

The boundaries $\partial\Omega_l$ and $\partial\Omega_r$ can be either clamped (LDBC) or linked (PBC). In case of LDBC the interface is not present. Evaluating the moment distribution when shearing this system leads to the two different functions for $\boldsymbol{\lambda}$.

3 Numerical Examples

The introduced additional constraints are tested on an U-shaped profile. Geometrical information are given in fig. 4a with $h = b = 10\ cm$, $s = 0.6\ cm$ and $t = 1.2\ cm$. To test the constraints, four types of RVE boundary conditions are chosen, namely PBC with a linked domain (PBCLink), PBC with the above given constraints eq. (4) (PBCConst), LDBC and LDBC with the constraint (LDBCConst). Figures 4b and 4c show the resulting shear correction factor over a varying length of the RVE. Here, PBCLink and PBCConst are truly length independent while LDBCConst converge against the same shear correction factor with increasing length. As in the previous example the shear correction factor for LDBC converges to zero and is unusable. The evaluation of the RVE leads to shear correction factors $\kappa_y = 0.6605$ and $\kappa_z = 0.1512$ compared to $\kappa_y = 0.6595$ and $\kappa_z = 0.1509$ calculated with the element in [1]. Regarding the cross sectional deformation,

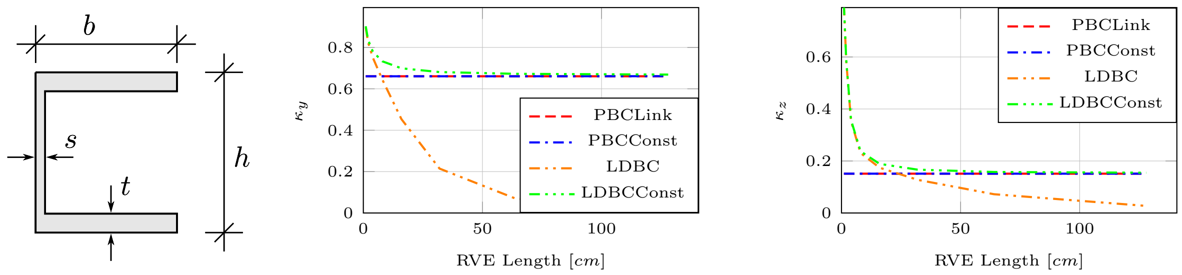

(a) Geometry **(b)** κ_y over RVE length **(c)** κ_z over RVE length

Figure 4. Shear correction factor – U-shaped profile

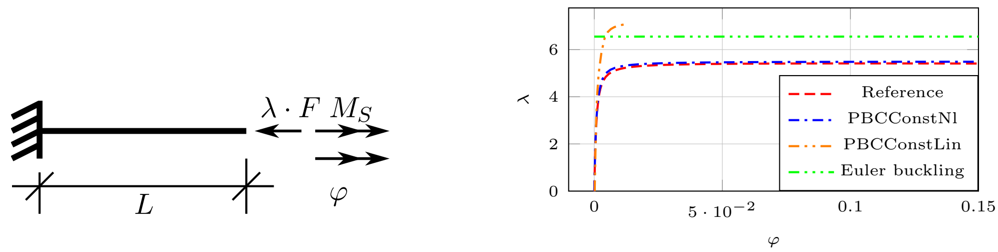

(a) System **(b)** Results

Figure 5. Example – Torsional buckling

the next example deals with torsional buckling. For this case material parameters are chosen as $E = 21000\ kN/cm^2$ and Poisson's ratio $\nu = 0.3$ while the cross-section stays the same as above. Figure 5a shows the system with $L = 150\ cm$, load $F = 100\ kN$ and a small imperfection $M_S = 0.1\ kNm$. The rotational degree of freedom φ is observed and results are depicted in fig. 5b. Geometrical non-linearity for the macro system is assumed, while the RVE is evaluated geometrically linear (PBCConstLin) and non-linear (PBCConstNl). Euler buckling is the critical load for the weak axis and the reference solution is evaluated with a geometrically non-linear 3D brick element. The results in case of a geometrically non-linear evaluation of the RVE agree very well with the reference solution, while the geometrically linear RVE is not able to represent torsional buckling. The reason for the overestimation of the Euler buckling case is the wrong imperfection.

Conclusion

A homogenization approach for the Timoshenko beam theory is presented with focus on shear stiffness. The introduced additional constraints make it possible to use pure periodic b.c. and get results independent of the RVE length. The resulting shear correction factors, and all other cross-sectional values, are length independent and agree with the reference solution. With a geometrical non-linear evaluation of the RVE the cross-sectional deformation is taken into account and it is possible to recognize the torsional buckling case.

References

[1] F. Gruttmann and W. Wagner. Shear correction factors in Timoshenko's beam theory for arbitrary shaped cross-sections. *Computational Mechanics*, 27(3):p. 199–207, 2001.

[2] F. Gruttmann and W. Wagner. A coupled two-scale shell model with applications to layered structures. *International Journal for Numerical Methods in Engineering*, 94(13):p. 1233–1254, 2013.